УДК 546.05+537.528
P.A.C.S. 52.80.Wq; 82.20.−w
DOI 10.54708/26587572_2023_5414135

SOME REGULARITIES OF PLASMA-SOLUTION SYNTHESIS OF BINARY OXIDE COMPOUNDS

Kristina Valerievna Smirnova [a], Polina Aleksandrovna Ivanova, Sergey Igorevich Kartashov, Dmitry Alexandrovich Shutov, Alexander Nikolaevich Ivanov, Vladimir Vladimirovich Rybkin

Ivanovo State University of Chemistry and Technology, Sheremetevsky pr. 7, 153000, Ivanovo, Russia
[a] smirnovakv1@gmail.com

ABSTRACT

In this paper, we consider the preparation of some double oxides of transition metals, namely $(ZnO)_{0.92}$ $(CdO)_{0.08}$, NiOCuO, $NiOCo_2O$, $CoFe_2O_4$, $NiFe_2O_4$, $ZnFe_2O_4$. The synthesis of bimetallic oxide compounds occurred in two stages. First, plasma-solution synthesis of ultrafine particles from solutions of a mixture of nitrates under the action of a DC glow discharge. The second was the high-temperature treatment of the resulting hydroxonitrates and hydroxides. The kinetics of the formation of the solid phase in the solution had an induction period associated with the accumulation of active particles in the solution under the action of the plasma and the change in the intensity of the light transmitted through the solution during the plasma treatment has an exponential decreasing character. The characteristic times of solid phase formation obtained from these dependences decrease with increasing discharge current. As a result of hydrolysis-like processes, hydroxides and hydroxonitrates of the corresponding metals were formed in the solution. This was confirmed by the XRD and EDS data. According to the data of a SEM and DLS, the particles obtained were characterized by two sizes: one was about 100 nm and the other was about 1.5 μm.

KEYWORDS

Double oxides; nanoparticles; gas discharge; SEM; kinetics.

НЕКОТОРЫЕ ЗАКОНОМЕРНОСТИ ПЛАЗМЕННО-РАСТВОРНОГО СИНТЕЗА ДВОЙНЫХ ОКСИДОВ

Кристина Валерьевна Смирнова [a], Полина Александровна Иванова, Сергей Игоревич Карташов, Дмитрий Александрович Шутов, Александр Николаевич Иванов, Владимир Владимирович Рыбкин

Ивановский государственный химико-технологический университет, Россия, 153000, Иваново, пр. Шереметевский, 7
[a] smirnovakv1@gmail.com

АННОТАЦИЯ

В данной работе рассмотрено получение некоторых двойных оксидов переходных металлов, а именно $(ZnO)_{0,92}$ $(CdO)_{0,08}$, NiOCuO, $NiOCo_2O$, $CoFe_2O_4$, $NiFe_2O_4$, $ZnFe_2O_4$. Синтез двойных

оксидных соединений происходит в две стадии. Во-первых, плазменно-растворный синтез ультрадисперсных частиц из растворов смеси нитратов под действием тлеющего разряда постоянного тока. Второй – высокотемпературная обработка полученных гидроксонитратов и гидроксидов. Полученные зависимости интенсивности прошедшего через раствор света во время плазменной обработки носят убывающий характер и описываются экспонентой. Характерные времена образования твердой фазы, полученные из этих зависимостей, уменьшаются с увеличением тока разряда. В результате гидролизоподобных процессов в растворе образуются гидроксиды и гидроксинитраты соответствующих металлов. Это подтвердили данные РСА и ЭДС. По данным СЭМ и ДРС полученные частицы характеризовались двумя размерами: один – 100 нм, другой – 1,5 мкм.

КЛЮЧЕВЫЕ СЛОВА

Двойные оксиды; наночастицы; газовый разряд; СЭМ; кинетика.

Introduction

Transition metal oxides with different morphology and composition are applicable in many spheres of human activity. Inorganic materials of this category meet all the requirements of modern industry and science standards and have a high priority for the study and development of advanced methods for their synthesis. Such particles include: $(ZnO)_{0.92}(CdO)_{0.08}$, NiOCuO, $NiOCo_2O$, $CoFe_2O_4$, $NiFe_2O_4$, $ZnFe_2O_4$. The presented compounds, and others from this group, have a variety of characteristics. It should be noted that individual metal oxides usually have poor conductive properties and low chemical stability, which limits their use. At the same time, binary oxide systems are free from this disadvantage. These materials are also unique in that their special physical and chemical properties, which depend directly on their size, can open up new areas of their application [1].

Bimetallic oxide compounds are used in biomedical engineering applications, where it is easy to use them to implement the so-called drug delivery [2] and multimodal imaging [3]. There are works on the detection of glucose using nanocrystals of oxides [4], as well as the identification of antibacterial activity [5].

The magnetic properties of such compounds are actively used in magnetic resonance imaging (MRI) [6]. Most of the nanocrystals are semiconductors with a high charge carrier density and different band structure, which allows the creation of band gaps for new applications. For example, ZnO nanorods are used as active components in lasers, and materials based on copper oxide play an important role in studies of high-temperature superconductivity [7]. In addition, in recent years there has been a tendency to use various carbon materials as anodes for lithium-ion batteries [8].

Of particular note are carbon fibers and fabrics, which have excellent flexibility and electrical conductivity. However, their significant disadvantage is their low specific capacitance. Therefore, in this case, it is impossible to do without applying layers of transition metal oxides to the surface of the carbon fabric, which are characterized by a high theoretical capacity, availability, and low cost. Therefore, the synthesis, study of the morphology and structural features of hybrids of transition metal oxides/carbon fabrics, as well as the study of the fundamental possibility of their use as anode materials for lithium-ion batteries, are among the urgent goals and objectives of many studies [8].

At present, the following synthesis methods are known for obtaining nanocrystals of transition metal oxides. Among them [1]: chemical vapor deposition [9], electrodeposition [10], sol-gel methods [11], hydrothermal methods [12], solvothermal methods [13], thermal decomposition methods [14], sonochemical methods [15], microwave methods [16], spray pyrolysis [17], and flame synthesis of aerosols [18]. Recently, oxide nanoparticles are mainly synthesized using environmentally friendly methods that are reproducible, simple, and economical. One of such methods for obtaining metal nanoparticles is a method based on the interaction of low-temperature gas-discharge plasma with solutions. The method is carried out using environmentally friendly solvents such as water, ionic liquids and supercritical fluids, using a minimum amount of substances.

Despite the fact that many different types of discharges and reactor designs have been proposed, all of them are united by the fact that the gas discharge plasma realized in them is nonequilibrium. The main role in initiating all chemical processes belongs to electrons. Their inelastic collisions with atoms and molecules of the plasma-forming gas lead to the formation of chemically active particles: atoms and molecules in excited states, radicals, positive and negative ions [19]. Their subsequent reactions with each other, as well as with substances that form the boundaries of the discharge, form the composition of the plasma.

Another specific feature is the fact that, in contrast to discharges limited by chemically inert walls (glass, ceramics, etc.), the evaporation of a solution into the gas phase strongly affects the properties of the plasma. The discharge always burns not in a pure gas, but in a gas with impurities of solution components. In fact, the chemical reactions that occur during the synthesis of nanoparticles in plasma-solution systems and are described by stoichiometric reaction equations are quite simple. They are based on the reduction of metal ions or semiconductors or the formation of insoluble compounds under the action of particles formed in solution under the action of plasma. The exception is when the formation occurs as a result of direct physical processes, such as cathode sputtering or reactive cathode sputtering.

The physical and chemical processes in the gas phase are being intensively studied by many researchers and technicians. However, active studies of physicochemical processes in plasma-solution systems began in recent decades due to the applications of these systems in water treatment [20–22], plasma medicine [23–26], synthesis of nanomaterials [27–33], etc.

Primary active particles in solution can appear in two ways. The first way is the diffusion of particles formed in the plasma into the solution. The second way is the formation of particles from water molecules under the action of bombardment of its surface by active agents of the discharge. There is no consensus in the literature and no direct experimental evidence as to which of the above paths is the main one. Thus, in a review paper [34] devoted to the synthesis of nanodispersed metal particles, it is believed that water molecules are ionized due to ion bombardment of the solution surface. The resulting electrons are the main reducing agents of metal cations ($Me^{n+}+ne \rightarrow M$). Experimentally, the fact of the formation of solvated electrons was discovered in [35]. A number of experimental facts also indicate that the second way is more probable. Thus, the formation of hydrogen peroxide is observed for discharges in all studied plasma-forming gases, including noble ones [36].

Over the past twenty years, studies on the interaction of plasma with solutions have described the nature of the formation of colloidal particles consisting of noble metals. However, the mechanisms of formation of particles in solutions under the action of gas

discharges containing one or more transition metal cations are still not completely clear. In this work, we have described some regularities in the formation of a solid phase in solutions containing two transition metal nitrates under the action of a glow discharge at atmospheric pressure in air. An additional motivation for studying these processes is the regulation of the composition and size of the obtained particles, as well as the fact that the final product of such synthesis are oxides containing two transition metal cations, which are promising in various fields of application.

1. Research Methods

The solutions were prepared by dissolving $M^{x+}(NO_3)^-_x$ (M = Zn^{2+}; Cd^{2+}; Cu^{2+}; Ni^{2+}; Co^{2+}; Fe^{3+}) (JSC "Himreactiv", Russia) in distilled water. The concentration of the working solution is shown in Table 1. The concentration was selected empirically so that the final ratio of metal cations corresponded to the compounds with the formula $(ZnO)_{0.92}(CdO)_{0.08}$, NiOCuO, $NiOCo_2O$, $CoFe_2O_4$, $NiFe_2O_4$, $ZnFe_2O_4$.

The discharge cell had an H-shape, divided into two identical parts by a cellophane membrane. The volume of each part was 100 ml. A high voltage was applied to titanium electrodes located at a distance of 5 mm from the surface of the solution, sufficient to ignite the plasma. After ignition of the gas discharge, the solution in the cell located under the metal anode became the liquid cathode, and the solution under the metal cathode became the liquid anode. The discharge current was 40 mA and the total input power was about 40 W. The setup scheme is described in more detail in [37]. By the action of a discharge a colloidal solution was formed in the near-surface layer of anode part of cell (A-cell) and precipitate was formed at the bottom of the cell. The obtained sol-like fraction from top of the A-cell was collected by pipette, centrifuged and rinsed with distilled water. Washed sol was dried in ambient air at 60 °C for 24 h.

The synthesis of bimetallic oxide compounds occurred in two stages. First, plasma-solution synthesis of ultrafine particles from solutions of a mixture of nitrates under the action of a DC glow discharge. The second was the high-temperature treatment of the resulting hydroxonitrates and hydroxides. The temperature was selected individually based on the data of thermogravimetric analysis and varied from 300 to 1000 °C depending on the metal cations used for the synthesis.

The kinetics of the colloidal particle formation process was investigated using the method of turbidimetry. The intensity of the light passing through the layer (1 mm below the surface) of the solution was measured with an AvaSpec-2048 FT-2 spectrometer (Avantes, Netherlands). The optical length was 45 mm. The light source was a He-Ne laser (λ = 632.8 nm).

The pH of the solution were measured before and after solution treatment using a PHT-028 multivariable water quality monitor (Kelilong, China).

Characterization of precipitates

For qualitative and quantitative analysis of the phase composition of the powders, x-ray diffraction analysis was used (x-ray diffractometer DRON 3 M, Burevestnik, Russia, CuKa radiation). The diffraction patterns were processed using QualX2 software [38] and the open crystallographic COD database [39].

Thermogravimetric analysis (TGA) and differential scanning calorimetry (DSC) of the obtained precipitates were performed on a STA 449 F1 Jupiter thermal analysis instrument (Netzsch, Germany). The temperature range was 20–900 °C at a heating rate of 5 °C min^{-1} in an argon flow using a platinum crucible.

The shape of the particles, their sizes and elemental composition of the powder were obtained using scanning electron microscopy (SEM, Tescan Vega 3SBH, Czech Republic) with an EDX analysis system (Aztec EDS, Oxford Instruments Ltd., England).

The average hydrodynamic diameter of the colloidal particles and their ʒ potential was determined by dynamic light scattering (DLS) using a Photocor Compact-Z size analyzer (Photocor, Russia).

2. Results and Discussion

Under the action of the discharge, no visible changes in the solution were observed during the first tens of seconds. After the induction period, the formation of colloidal particles in the solution began in the region of the plasma-solution contact in the anode part of the cell. In this case, the formation of particles in the cathode part of the cell was not observed. Turbidimetric curves are well described by two exponents (Fig. 1). Such processing makes it possible to determine the effective rate constants or characteristic times. The dependences of the change in the rate constants of the formation of the solid phase on the discharge current for the second section are shown in Fig. 2. As it can be seen from the graph, the rate of formation of the solid phase in the solution under the action of the discharge increases with increasing current. This is directly related to the accumulation of active particles in the solution under the action of the discharge.

The results of XRD and EDS analysis of the composition of substances obtained from colloidal particles showed that these are mixtures of crystalline hydroxonitrates and hydroxides of the corresponding metals (Table 1). The formation of these compounds requires a certain concentration of hydroxide OH- ions, that is, it depends on the pH of the solution. The initial solutions of the studied salts had an acidic environment due to the hydrolysis of salts (Table 1). For a solution containing only one type of metal ion, there is an increase in pH in the liquid anode (an increase in the concentration of OH- ions) with the treatment time and a decrease in the liquid cathode (a decrease in the concentration of OH- ions). In the case of solutions of mixtures of salts, a strong change in the pH of the solution is not observed even after 10 minutes of treatment (Fig. 3).

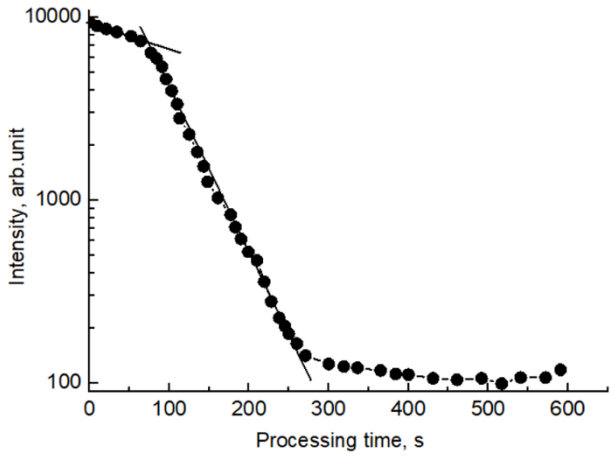

Fig. 1. The dependence of the normalized transmission of the solution on the processing time for a mixture of zinc and cadmium nitrates [40].
Discharge current is 70 mA

Рис. 1. Зависимость интенсивности прошедшего через раствор света от времени обработки для смеси нитратов цинка и кадмия [40].
Ток разряда 70 мА

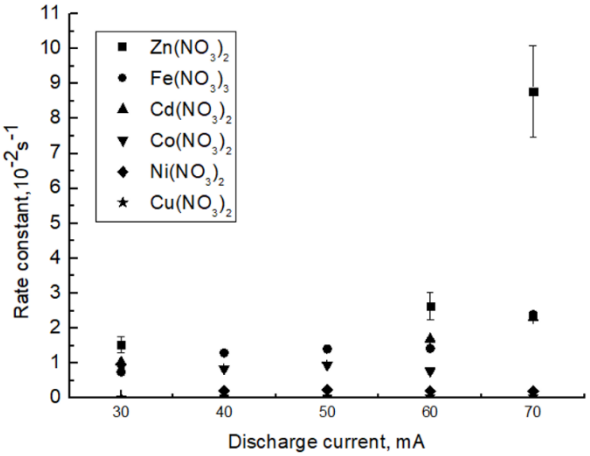

Fig. 2. The dependence of the effective rate constants on the discharge current. Initial concentration of nitrates 5 mmol/l

Рис. 2. Зависимость эффективных констант скорости от тока разряда. Исходная концентрация нитратов 5 ммоль/л

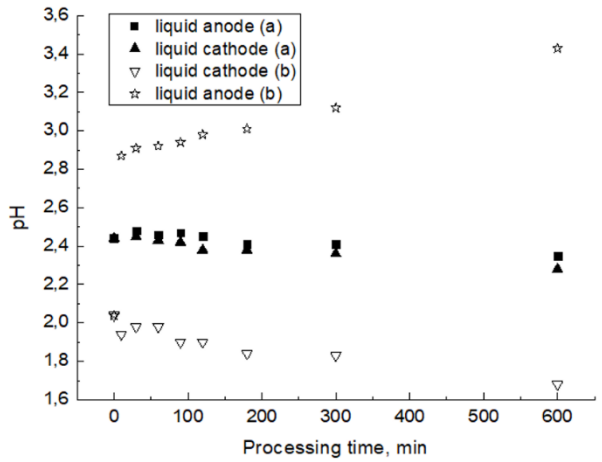

Fig. 3. Kinetics of change in the pH of the solution vs the time of plasma treatment:
a – mixture of iron nitrate and cobalt nitrate (initial concentrations of iron nitrate 3 mmol/l and cobalt nitrate 50 mmol/l); b – iron nitrate (initial concentration of iron nitrate 5 mmol/l). Discharge current is 40 mA

Рис. 3. Кинетика изменения pH раствора в зависимости от времени плазменной обработки:
а – смесь нитрата железа и нитрата кобальта (начальные концентрации нитрата железа 3 ммоль/л и нитрата кобальта 50 ммоль/л); б – нитрат железа (исходная концентрация нитрата железа 5 ммоль/л). Ток разряда 40 мА

The calculation using the solubility products (Table 1) shows that the formation of insoluble hydroxides and hydroxonitrates at the measured pH values in the cathode cell is thermodynamically impossible. It should be noted that the results of pH measurements are averaged over the cell volume, and the main changes in pH occur in a thin near-surface layer. In both cases, the thickness of these layers is several nanometers. For this reason, the environment directly in the reaction zone in the cathode part should be more acidic, and in the anode part – more alkaline compared to the experimentally measured ones.

Table 1. Oxide metal particles synthesis in plasma solution system. Discharge current 40 mA

Таблица 1. Оксиды металлов синтезированные в плазменно-растворной системе. Ток разряда 40 мА

Type of particles after calcination	Raw materials of solutions	Initial concentration, mmol/l	Solubility product	pH deposition of metal hydroxides	XRD and EDS of precursor
$(ZnO)_{0.92}(CdO)_{0.08}$	$Zn(NO_3)_2$	50	$1.2\cdot10^{-17}$	6.4	$Zn(NO_3)OH\cdot H_2O$, $Zn(OH)_2$, γ-$Cd(OH)_2$, β-$Cd(NO_3)OH\cdot H_2O$
	$Cd(NO_3)_2$	50	$2\cdot10^{-19}$	8.2	
$CoFe_2O_4$	$Co(NO_3)_2$	50	$1.6\cdot10^{-15}$	7.6	$Co(NO_3)OH\cdot H_2O$, $Co(OH)_2$, $Fe(OH)_3$, $Fe(NO_3)_2OH\cdot H_2O$
	$Fe(NO_3)_3$	3	$6.3\cdot10^{-38}$	2.3	
$NiFe_2O_4$	$Ni(NO_3)_2$	50	$2.0\cdot10^{-15}$	7.7	$Ni(NO_3)OH\cdot H_2O$, $Ni(OH)_2$, $Fe(OH)_3$, $Fe(NO_3)_2OH\cdot H_2O$
	$Fe(NO_3)_3$	2.5	$6.3\cdot10^{-38}$	2.3	
$ZnFe_2O_4$	$Zn(NO_3)_2$	50	$1.2\cdot10^{-17}$	6.4	$Zn(NO_3)OH\cdot H_2O$, $Zn(OH)_2$, $Fe(OH)_3$, $Fe(NO_3)_2OH\cdot H_2O$
	$Fe(NO_3)_3$	4	$6.3\cdot10^{-38}$	2.3	
NiOCuO	$Ni(NO_3)_2$	50	$2.0\cdot10^{-15}$	7.7	$Ni(NO_3)OH\cdot H_2O$, $Ni(OH)_2$, $Cu(OH)_2$, $Cu(NO_3)OH\cdot H_2O$
	$Cu(NO_3)_2$	2	$2.2\cdot10^{-20}$	5.3	
NiOCoO	$Ni(NO_3)_2$	25	$2.0\cdot10^{-15}$	7.7	$Ni(NO_3)OH\cdot H_2O$, $Ni(OH)_2$, $Co(OH)_2$, $Co(NO_3)OH\cdot H_2O$
	$Co(NO_3)_2$	50	$6.3\cdot10^{-38}$	2.3	

The reasons for the different pH values for the liquid cathode and anode are that the surface of the liquid anode, unlike the cathode, is bombarded by plasma electrons [41, 42]. As a result, the electron concentration in a surface layer several nanometers thick reaches a value of about 1 mmol/L. These electrons react very quickly with water molecules to form hydroxide ions (Fig. 4). This leads to higher pH values in the anode cell compared to the cathode. An increase in the discharge current leads to an increase in the electron flux from the plasma, the rate of formation of hydroxide ions OH- and, as a consequence, the rate of formation of colloidal particles. This is reflected in an increase in the effective rate constant with an increase in the discharge current (Fig. 2).

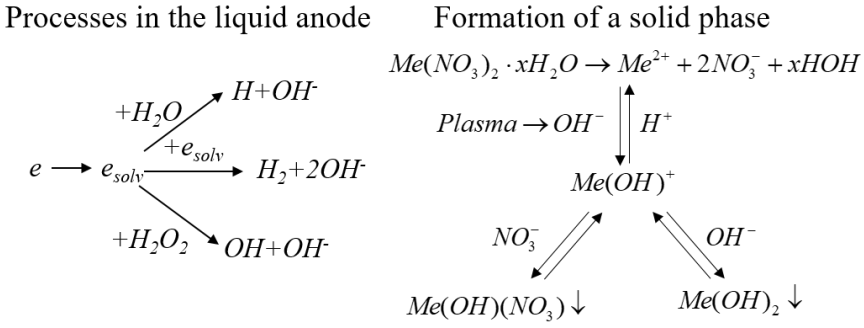

Fig. 4. Mechanisms of formation of a solid phase under the action of a low-temperature, nonequilibrium plasma initiated by the action of a DC glow discharge on an aqueous solution

Рис. 4. Механизмы образования твёрдой фазы в водном растворе под действием низкотемпературной неравновесной плазмы, инициируемой воздействием тлеющего разряда постоянного тока

The results of quantitative determination of the composition of the solid phase obtained from mixtures of salts showed that the ratio of the components did not correspond to their ratio in solution. Even with an equal molar ratio in solution, the concentration of the metal in the solid phase is the greater, the smaller the solubility product for the corresponding insoluble compound. That is, the substance with the lowest value of the solubility product begins to form first. This fact must be taken into account in order to obtain a compound of the desired composition. High-temperature treatment of the resulting powders leads to the formation of the corresponding oxides.

All obtained powders had a well-developed surface and their images obtained on a scanning electron microscope are shown in Fig. 5. All samples are characterized by the presence of agglomerates approximately 1.5 μm in size. Their presence is explained by van der Waals forces, and in the case of iron-containing particles, by the magnetic properties of these materials. The resulting colloidal particles were also studied using the method of dynamic light scattering. All samples are characterized by a clear distribution into two characteristic fractions. The first 40% is 100±10 nm, and the second 60% is 1.5 μm.

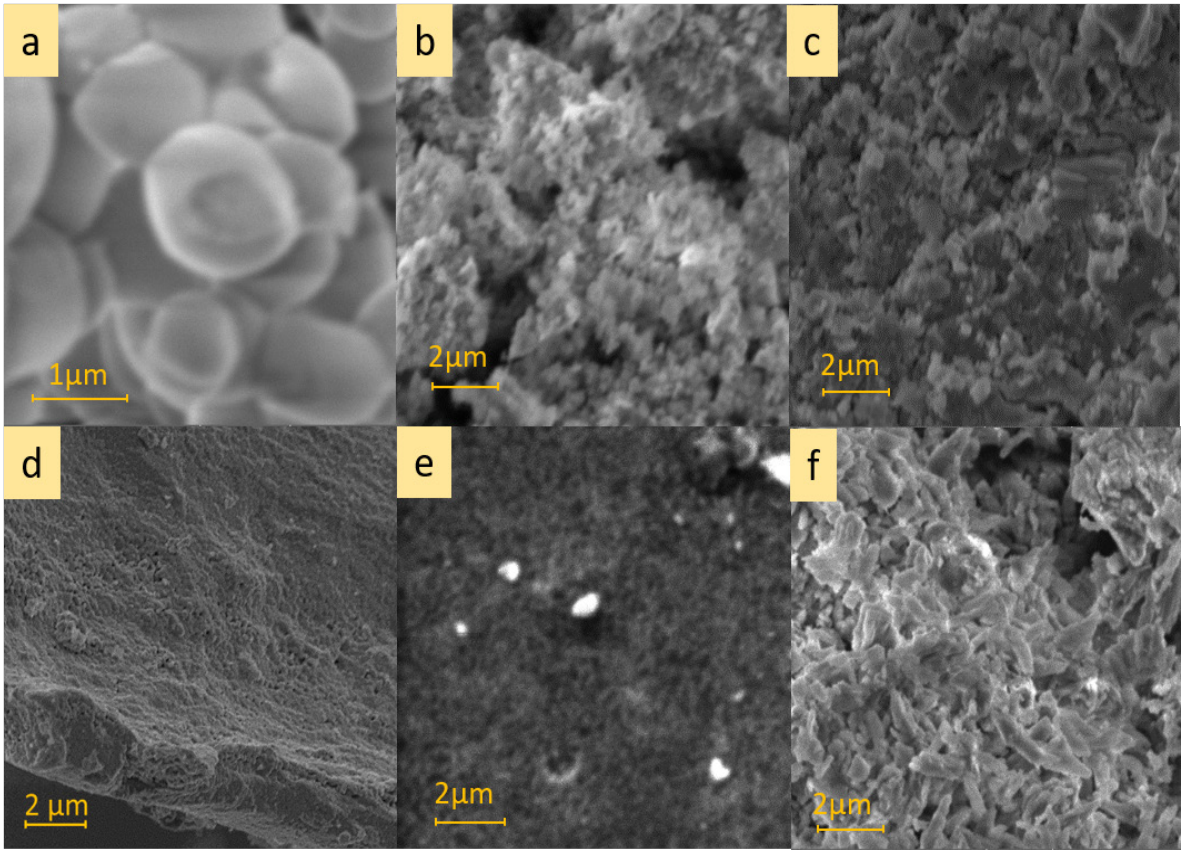

Fig. 5. SEM image of calcined synthesized powder:
a – $(ZnO)_{0.92}$ $(CdO)_{0.08}$; b – $NiOCuO$; c – $NiOCo_2O$; d – $CoFe_2O_4$; e – $NiFe_2O_4$; f – $ZnFe_2O_4$

Рис. 5. Изображения, полученные на СЭМ синтезированного порошка после высокотемпературной обработки:
a – $(ZnO)_{0,92}(CdO)_{0,08}$; b – $NiOCuO$; c – $NiOCo_2O$; d – $CoFe_2O_4$; e – $NiFe_2O_4$; f – $ZnFe_2O_4$

Conclusions

The work shows the possibility of synthesizing ultrafine oxide materials from solutions of nitrate mixtures under the action of a nonequilibrium gas-discharge plasma. A gas discharge is a source of a large number of active particles, but the main contribution to the formation of a solid phase in a solution under the action of a discharge is made by electrons, in the reactions of which hydroxide ions are formed with water molecules. The reactions of these ions lead to the formation of insoluble hydroxonitrates and hydroxides of the corresponding metals. High temperature treatment of these compounds transforms them into mixed oxides $(ZnO)_{0.92}(CdO)_{0.08}$, NiOCuO, $NiOCo_2O$, $CoFe_2O_4$, $NiFe_2O_4$, $ZnFe_2O_4$.

Acknowledgments / Благодарности

This work was supported the partial financial support of the Ministry of High Education and Science of the Russian Federation, project No. FZZW-2023-0010.

K. Smirnova is grateful for the financial support of the grant of the Russian Federation President (MK-2607.2022.1.2).

The study was carried out using the resources of the Center for Shared Use of Scientific Equipment of the Ivanovo State University of Chemistry and Technology (with the support of the Ministry of Science and Higher Education of Russia, No. 075-15-2021-671).

Работа выполнена при частичной финансовой поддержке Минобрнауки РФ, проект № FZZW-2023-0010.

Смирнова К. благодарит за финансовую поддержку грант Президента РФ (МК-2607.2022.1.2).

Исследование проведено с использованием ресурсов Центра коллективного пользования научного оборудования ИГХТУ (при поддержке Минобрнауки России, № 075-15-2021-671).

REFERENCES

1. Qiao L., Swihart M. T. Solution-phase synthesis of transition metal oxide nanocrystals: Morphologies, formulae, and mechanisms // Advances in Colloid and Interface Science. 2017. V. 244. P. 199–266. DOI: 10.1016/j.cis.2016.01.005.

2. Fan W., Bu W., Shen B., He Q., Cui Z., Liu Y., Zheng X., Zhao K., Shi J. Intelligent MnO_2 nanosheets anchored with upconversion nanoprobes for concurrent pH-/H_2O_2-responsive UCL imaging and oxygen-elevated synergetic therapy // Advanced Materials. 2015. V. 27, Iss. 28. P. 4155–4161. DOI: 10.1002/adma.201405141.

3. Liu T., Shi S., Liang C., Shen S., Cheng L., Wang C., Song X., Goel S., Barnhart T. E., Cai W., Liu Z. Iron oxide decorated MoS2 nanosheets with double PEGylation for chelator-free radiolabeling and multimodal imaging guided photothermal therapy // ACS nano. 2015. V. 9, Iss. 1. P. 950–960. DOI: 10.1021/nn506757x.

4. Hui N., Wang J. Electrodeposited honeycomb-like cobalt nanostructures on graphene oxide doped polypyrrole nanocomposite for high performance enzymeless glucose sensing // Journal of Electroanalytical Chemistry. 2017. V. 798. P. 9–16. DOI: 10.1016/j.jelechem.2017.05.021.

5 Ma C., Wang W., Kong D., Wei S., Li W., Chen S. A novel core/shell cuprous oxide-based structure with improved microwave absorbing and antibacterial performance // Journal of Cleaner Production. 2022. V. 378. Article number 134419. DOI: 10.1016/j.jclepro.2022.134419.

6. Zhao Z., Li M., Zeng J., Huo L., Liu K., Wei R., Ni K., Gao J. Recent advances in engineering iron oxide nanoparticles for effective magnetic resonance imaging // Bioactive Materials. 2022. V. 12. P. 214–245. DOI: 10.1016/j.bioactmat.2021.10.014.

7. Wei X., Li H.-B., Zhang Q., Li D., Qin M., Xu L., Hu W., Huan Q., Yu L., Miao J., Yuan J., Zhu B., Kusmartseva A., Kusmartsev F. V., Silhanek A. V., Xiang T., Yu W., Lin Y., Gu L., Yu P., Jin K. A selective control of volatile and non-volatile superconductivity in an insulating copper oxide via ionic liquid gating // Science Bulletin. 2020. V. 65, Iss. 19. P. 1607–1613. DOI: 10.1016/j.scib.2020.05.013.

8. Khramenkova A. V., Moshchenko V. V., Yakovenko A. A., Pushnitsa K. A., Pavlovskii A. A., Maximov M. Yu. Synthesis, structure investigation and future prospects of transition metal oxides/carbon cloth hybrids as flexible binder-free anode materials for lithium-ion batteries // Materials Letters. 2022. V. 329. Article number 133250. DOI: 10.1016/j.matlet.2022.133250.

9. van Mol A. M. B., Chae Y., McDaniel A. H., Allendorf M. D. Chemical vapor deposition of tin oxide: Fundamentals and applications // Thin Solid Films. 2006. V. 502, Iss. 1–2. P. 72–78. DOI: 10.1016/j.tsf.2005.07.247.

10. Li M., Jijie R., Barras A., Roussel P., Szunerits S., Boukherroub R. NiFe layered double hydroxide electrodeposited on Ni foam coated with reduced graphene oxide for high-performance supercapacitors // Electrochimica Acta. 2019. V. 302. P. 1–9. DOI: 10.1016/j.electacta.2019.01.187.

11. Hasan S., Azhdar B. $NiFe_2O_4$ and $ZnFe_2O_4$ nanoparticles synthesis by sol-gel auto-combustion for humidity sensor applications // J Sol-Gel Sci Technol. 2023. V. 105. P. 416–429. DOI: 10.1007/s10971-023-06039-4.

12. Farid H. M. T., Gouadria S., Al-Moayid S. M., Algarni H., Ansari M. Z., Ali H. E. Facile synthesis of CuCo2O4 spinel with rGO nanocomposite via hydrothermal approach for solid state supercapacitor application // Journal of Energy Storage. 2023. V. 66. Article number 107394. DOI: 10.1016/j.est.2023.107394.

13. Duong H. D. T., Nguyen D. T., Kim K.-S. Effects of Process Variables on Properties of $CoFe_2O_4$ Nanoparticles Prepared by Solvothermal Process // Nanomaterials. 2021. V. 11, Iss. 11. Article number 3056. DOI: 10.3390/nano11113056.

14. L'vov B. V. The physical approach to the interpretation of the kinetics and mechanisms of thermal decomposition of solids: the state of the art // Thermochimica Acta. 2001. V. 373, Iss. 2. P. 97–124. DOI: 10.1016/S0040-6031(01)00507-X.

15. Kummari S. V., Srikanth V. V. S. S. CoFe content-controlled magnetic exchange coupling in $CoFe_2O_4$-CoFe composites prepared by a simple and single-step sonochemical reduction method // Materials Letters. 2023. V. 347. Article number 134626. DOI: 10.1016/j.matlet.2023.134626.

16. Zhang Y., Zheng J., Nan J., Gai C., Shao Q., Murugadoss V., Maganti S., Naik N., Algadi H., Huang M., Xu B. B., Guo Z. Influence of mass ratio and calcination temperature on physical and photoelectrochemical properties of ZnFe-layered double oxide/cobalt oxide heterojunction semiconductor for dye degradation applications // Particuology. 2023. V. 74. P. 141–155. DOI: 10.1016/j.partic.2022.05.010.

17. Gautam S., Thakur P., Bazylewski P., Bauer R., Singh A. P., Kim J. Y., Subramanian M., Jayavel R., Asokan K., Chae K. H., Chang G. S. Spectroscopic study of Zn1−xCoxO thin films showing intrinsic ferromagnetism // Materials Chemistry and Physics. 2013. V. 140, Iss. 1. P. 130–134. DOI: 10.1016/j.matchemphys.2013.03.011.

18. Li S., Ren Y., Biswas P., Tse S. D. Flame aerosol synthesis of nanostructured materials and functional devices: Processing, modeling, and diagnostics // Progress in Energy and Combustion Science. 2016. V. 55. P. 1–59. DOI: 10.1016/j.pecs.2016.04.002.

19. Elg D. T., Delgado H. E., Martin D. C., Sankaran R. M., Rumbach P., Bartels D. M., Go D. B. Recent advances in understanding the role of solvated electrons at the plasma-liquid interface of solution-based gas discharges // Spectrochimica Acta, Part B: Atomic Spectroscopy. 2021. V. 186. Article number 106307. DOI: 10.1016/j.sab.2021.106307.

20. Rybkin V. V., Smirnov S. A., Titov V. A., Arzhakov D. A. The characteristics of electrons and vibrational distributions of molecules in an atmospheric-pressure liquid-cathode dc discharge in air // High Temp. 2010. V. 48. P. 476–481. DOI: 10.1134/S0018151X10040036.

21. Hofmann S., van Gessel A. F. H., Verreycken T., Bruggeman P. J. Power dissipation, gas temperatures and electron densities of cold atmospheric pressure helium and argon RF plasma jets // Plasma Sources Sci. and Technol. 2011. V. 20, Iss. 6. Article number 065010. DOI: 10.1088/0963-0252/20/6/065010.

22. Nikiforov A. Yu., Leys Ch., Gonzalez M. A., Walsh J. L. Electron density measurement in atmospheric pressure plasma jets: Stark broadening of hydrogenated and non-hydrogenated lines // Plasma Sources Sci. and Technol. 2015. V. 24, Iss. 3. Article number 034001. DOI: 10.1088/0963-0252/24/3/034001.

23. Chen Q., Li J., Li Y. A review of plasma–liquid interactions for nanomaterial synthesis // J. Phys. D: Appl. Phys. 2015. V. 48, Iss. 42. Article number 424005. DOI: 10.1088/0022-3727/48/42/424005.

24. Chen Q., Kaneko T., Hatakeyama R. Synthesis of Superfine Ethanol-Soluble CoO Nanoparticles via Discharge Plasma in Liquid // Appl. Phys. 2012. V. 5, Iss. 9. Article number 096201. DOI: 10.1143/APEX.5.096201.

25 Gangal U., Srivastava M., Sen Gupta S. K. Scavenging effects of aliphatic alcohols and acetone on H· radicals in anodic contact glow discharge electrolysis: determination of the primary yield of H• Radicals // Plasma Chem. Plasma Process. 2010. V. 30, Iss. 2. P. 299–309. DOI: 10.1007/s11090-010-9216-9.

26. Singh R., Gangal U., Sen-Gupta S. K. Effects of Alkaline Ferrocryanide on Non-faradaic Yields of Anodic Contact glow Discharge electrolysis: Determination of the Primary Yield of OH· Radicals // Plasma Chem. Plasma Process. 2012. V. 32, Iss. 3. P. 609–617. DOI: 10.1007/s11090-012-9361-4.

27. Acayanka E., Tiya Djowe A., Laminsi S., Tchoumkwé C. C., Nzali S., Mbouopda A. P., Ndifon P. T., Gaigneaux E. M. Plasma-assisted synthesis of TiO_2 nanorods by gliding arc discharge processing at atmospheric pressure for photocatalytic applications // Plasma Chem. and Plasma Process. 2013. V. 33, Iss. 4. P. 725–735. DOI: 10.1007/s11090-013-9455-7.

28. Abdullaeva Z., Omurzak E., Iwamot C., Ganapathy H. S., Sulaimankulova S., Liliang C., Mashimo T. Onion-like carbon-encapsulated Co, Ni,

and Fe magnetic nanoparticles with low cytotoxicity synthesized by a pulsed plasma in a liquid // Carbon. 2012. V. 50, Iss. 5. P. 1776–1785. DOI: 10.1016/j.carbon.2011.12.025.

29. Kelgenbaeva Zh., Omurzak E., Takebe S., Abdullaeva Zh., Sulaimankulova S., Iwamoto C., Mashimo T. Magnetite nanoparticles synthesized using pulsed plasma in liquid // Jpn. J. Appl. Phys. 2013. V. 52, Iss. 11S. Article number 11NJ02. DOI: 10.7567/JJAP.52.11NJ02.

30. Omurzak E., Shimokawa W., Taniguchi K., Chen L.,Okamoto M., Iwasaki H., Yamasaki M., Kawamura Y., Sulaimankulova S., Mashimo T. Synthesis of wurtzite-type ZnMgS by the pulsed plasma in liquid // Jpn. J. Appl. Phys. 2011. V. 50, Iss. 1S1. Article number 01AB09. DOI: 10.1143/JJAP.50.01AB09.

31. Bera D., Kuiry S. C., McCutchen M., Seal S., Heinrich H., Slane G. C. In situ synthesis of carbon nanotubes decorated with palladium nanoparticles using arc-discharge in solution method // J. Appl. Phys. 2004. V. 96, Iss. 9. P. 5152–5157. DOI: 10.1063/1.1786347.

32. Sergiienko R., Shibata E., Zentaro A., Shindo D., Nakamura T., Qin G. Formation and characterization of graphite encapsulated cobalt nanoparticles synthesized by electric discharge in an ultrasonic cavitation field of liquid ethanol // Acta Mater. 2007. V. 55, Iss. 11. P. 3671–3680. DOI: 10.1016/j.actamat.2007.02.017.

33. Adamovich I., Agarwal S., Ahedo E., Alves L. L., Baalrud S., Babaeva N., Bogaerts A., Bourdon A., Bruggeman P. J., Canal C. The 2022 Plasma Roadmap: low temperature plasma science and technology // J. Phys. D: Appl. Phys. 2022. V. 55, No. 37. Article number 373001. DOI: 10.1088/1361-6463/ac5e1c.

34. Kaneko T., Baba K., Harada T., Hatakeyama R. Novel Gas-Liquid Interfacial Plasmas for Synthesis of Metal Nanoparticles // Plasma Process. and Polym. 2009. V. 6, Iss. 11. P. 713–718. DOI: 10.1002/ppap.200900029.

35. Richmonds C., Sankaran R. M. Plasma-liquid electrochemistry: rapid synthesis of colloidal metal nanoparticles by microplasma reduction of aqueous cations // Appl. Phys. Lett. 2008. V. 93, Iss. 13. Article number 131501. DOI: 10.1063/1.2988283.

36. Locke B. R., Shih K.-Y. Review of the methods to form hydrogen peroxide in electrical discharge plasma with liquid water // Plasma Sources Sci. Technol. 2011. V. 20, No. 3. Article number 034006. DOI: 10.1088/0963-0252/20/3/034006.

37. Shutov D. A., Ivanov A. N., Rakovskaya A. V., Smirnova K. V., Manukyan A. S., Rybkin V. V. Synthesis of oxygen-containing iron powders and water purification from iron ions by glow discharge of atmospheric pressure in contact with the solution // J. Phys. D: Appl. Phys. 2020. V. 53. Article number 445202. DOI: 10.1088/1361-6463/aba4d7.

38. Altomare A., Corriero N., Cuocci C., Falcicchio A., Moliterni A., Rizzi R. QUALX2.0: a qualitative phase analysis software using the freely available database POW_COD // J. Appl. Cryst. 2015. V. 48. P. 598–603. DOI: 10.1107/S1600576715002319.

39. Grazulis S., Daskevic A., Merkys A., Chateigner D., Lutterotti L., Quirós M., Serebryanaya N. R., Moeck P., Downs R. T., Bail A. L. Crystallography Open Database (COD): an open-access collection of crystal structures and platform for world-wide collaboration // Nucleic Acids Res. 2012. V. 40, Iss. D1. P. 420–427. DOI: 10.1093/nar/gkr900.

40. Smirnova K. V., Shutov D. A., Ivanov A. N., Manukyan A. S., Rybkin V. V. Plasma-Solution Synthesis of Zinc Oxide Doped with Cadmium. // ChemChemTech. 2022. V. 65, Iss. 7. P. 28–34. DOI: 10.6060/ivkkt.20226507.6629.

41. Shutov D. A., Batova N. A., Smirnova K. V., Ivanov A. N., Rybkin V .V. Kinetics of processes initiated in a water cathode by the action of a direct current discharge at atmospheric pressure in air: simulation and experiment // Journal of Physics D: Applied Physics. 2022. V. 55, No. 34. Article number 345206. DOI: 10.1088/1361-6463/ac74f8.

42. Shutov D. A., Smirnova K. V., Ivanov A. N., Rybkin V. V. The Chemical Composition of Species Formed in a Water Anode under the Action of a Direct Current Electric Discharge: Comparison with Liquid Cathode–Experiment and Simulation // Plasma Chemistry and Plasma Processing. 2023. V. 43, Iss. 3. P. 577–597. DOI: 10.1007/s11090-023-10322-1.